JASA ARTICLE

An adaptive algorithm for acoustic feedback compensation and secondary path identification of an active noise control system

Zhu Jie Feng,[1] Tian Ran Lin,[1,a)] and Li Cheng[2]
[1]Qingdao Key Rail Transportation Centre for Noise and Vibration Control & Automated Fault Diagnostic, Qingdao University of Technology, China
[2]Department of Mechanical Engineering, Hong Kong Polytechnic University, Hong Kong, China

ABSTRACT:
An adaptive variable step-size algorithm is proposed in this paper to address the impact of the real-time acoustic feedback and the real-time secondary path identification on the overall noise reduction performance of an active noise control system. An automated adjustment weight factor is introduced in the algorithm to accelerate the convergence of the acoustic feedback path as well as the secondary path identification, and to prevent possible system divergence. It is shown in this study that the proposed algorithm can resolve the trade-off between a fast convergence and a low misalignment of the virtual and the actual control paths typically found in conventional algorithms. An optimized control structure is also proposed in the study by enabling an adaptive gain adjustment based on the output of the auxiliary filter to enhance the practicality of the control system. The effectiveness of the algorithm is tested using two simulated multi-component signals and a broadband noise signal, and the results confirm that the proposed algorithm can achieve a good noise reduction with only a few iterations. © *2023 Acoustical Society of America*.
https://doi.org/10.1121/10.0022574
(Received 12 July 2023; revised 10 November 2023; accepted 10 November 2023; published online 19 December 2023)
[Editor: Mingsian R. Bai] Pages: 3851–3867

I. INTRODUCTION

Noise control techniques can be generally grouped into two categories, passive noise control and active noise control (ANC). Passive noise control can be achieved by means of noise absorption or noise isolation, while ANC can be achieved by the cancellation of the original noise source using an out-of-phase secondary sound source generated by an active control system.[1–3] ANC has gained immense attention from researchers since its inception and has been widely adopted in many practical engineering applications such as noise reduction in the incubator of neonatal children intensive care units,[4] noise reduction in nuclear magnetic imaging,[5] and noise reduction in heating, ventilation, and air-conditioning (HVAC) systems.[6] ANC systems can also be classified into two classes according to the design of the control loops, feedforward, and feedback systems. A feedforward system can have a better noise reduction performance than a feedback system, as it uses an additional reference microphone to capture detailed information of the incoming noise signal and incorporates it into the control algorithm. However, a feedforward system often faces the challenge of acoustic feedback and secondary path identification during the implementation. This then motivates the work presented in this study where an adaptive variable step-size algorithm is proposed to reduce the impact of the acoustic feedback and to increase the accuracy and convergence speed of the secondary path identification.

A schematic illustration of a feedforward system is shown in Fig. 1, where a reference microphone is used to monitor the incoming noise signal $x(n)$ and an error microphone is utilized to measure the error signal $e(n)$ after the cancellation between the control signal and the primary signal in which n signifies the time step. Also, shown in Fig. 1, $d(n)$ is the noise source signal after it propagates through the primary path $\mathbf{P}(z)$, and $\hat{d}(n)$ is the anti-noise signal after the control signal $y(n)$ passes through the secondary path $\mathbf{S}(z)$. The control signal $y(n)$ is generated by a loudspeaker based on the monitored source signal $x(n)$ using the filter-x least mean square algorithm (FxLMS).[7–9] It is shown in the figure that the control signal will not only propagate through the secondary path $\mathbf{S}(z)$, it can also be picked up by the reference microphone via the acoustic feedback loop described by $\mathbf{F}(z)$ which will then form a closed loop leading to system instability. Therefore, it is necessary to develop an algorithm to eliminate the effect of this acoustic feedback path $\mathbf{F}(z)$ in the control system.[10–12]

The acoustic feedback problem can be addressed by the implementation of a feedback neutralization algorithm involving the establishment of a compensation filter to counteract the acoustic feedback signal.[13] This can be realized by generating an auxiliary noise signal at the output of $\mathbf{W}(z)$, and then a time-varying transfer function $\hat{\mathbf{F}}(z)$[10,14–16] can be estimated in real-time to compensate for the acoustic feedback. The neutralization algorithms presented in several studies[13,15,16] use a fixed gain auxiliary noise and a fixed step control algorithm. However, it is found that even at the convergence stage of the control algorithm, the auxiliary

a)Email: trlin@qut.edu.cn

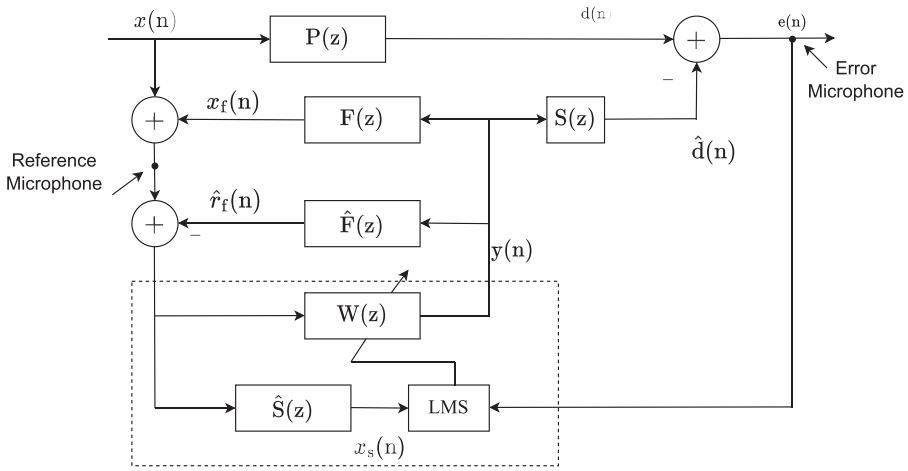

FIG. 1. A typical feedforward ANC system with an acoustic feedback loop.

loop still injects the auxiliary noise into the system leading to the instability of the control system, whereas Ahmed *et al.*[14] proposed an improved algorithm by including a gain control schedule to adjust the output of the auxiliary noise to stabilize the system, though it is found that the system has a slow convergence rate and the system can still be instabilized due to the use of a fixed step algorithm. To further address this issue, Ahmed *et al.*[17] introduced a variable step-size least mean square algorithm (VSSLMS) algorithm for a single-channel ANC system to speed up the system convergence. Nonetheless, many parameters are used in the algorithm which need to be regulated manually rendering a high uncertainty in the control outcome. On the other hand, Aslam *et al.*[18] added a norm calculation module based on the variable gain algorithm to avoid excessive updating caused by an excessive change in the acoustic feedback. In their approach, a linear predictive filter was used in the control loop to filter the input noise for better accuracy in the estimation of the acoustic feedback. However, the input signal needs to be known before the algorithm can be implemented. In contrast, the incoming signal in an actual industrial environment is difficult to predict beforehand. To address this issue, Akhtar *et al.*[19] proposed another improved algorithm by eliminating the linear predictive filter from the control system and modifying the feedback compensation path loop. Yet, the fixed step algorithm used in their approach can still lead to a slow convergence speed in addition to the inherent risk of system divergence due to the continuous injection of auxiliary noise into the system. Aiming to resolve this drawback, this paper presents an improved iterative algorithm by using an adaptive variable step-size algorithm together with an adaptive adjustment weight factor to speed up the system convergence as well as to prevent the occurrence of system divergence.

In an ANC system, the secondary path refers to the physical path linking the actuator to the error sensor which comprises three main components, the electronic circuit, the actuator, and the error microphone. The control error from the secondary path is mainly due to the time delay when the control signal passes through the electronic circuit and the actuator.[20] Thus, an accurate identification of the secondary path is crucial to minimize the phase error of a control signal for good noise control performance. Existing secondary path identification techniques can be grouped into two categories: offline identification and online (real-time) identification. Offline identification is commonly employed in conventional ANC systems.[21] However, the identification technique can only be applied to a fixed signal transmission path where an inaccurate result can be produced when the signal transmission path varies. As a result, online identification is more popular in modern ANC systems for a more accurate secondary path identification to ensure a stable and reliable control system performance.[22]

Online secondary path identification algorithms can be divided into two classes, non-auxiliary signal injection,[23] and auxiliary signal injection,[24] though it has been proved that a secondary path identification with auxiliary signal injection will have a better control performance.[24–26] Eriksson *et al.*[24] injected an auxiliary signal into the secondary path identification for the first time to realize a better accuracy in the second path identification. However, the auxiliary signal was also injected into the control filter in their approach leading to the divergence of the control filter. Moreover, the signal from the primary path can also propagate downstream to the secondary path identification filter to affect the accuracy of the secondary path identification as the number of iterations of the algorithm increases. Bao *et al.*[27] introduced a third auxiliary filter to solve the effect of the primary path on the identification process, though it does not resolve the interference of the auxiliary signal on the control filter. Zhang and Lan[28] used a similar auxiliary filter and an optimizing system control loop to overcome the deficiency of Eriksson and Allie's algorithm. Nevertheless, it has been noted that the inclusion of the auxiliary filter and the use of the fixed-step algorithm in the secondary path identification will lead to an increased computation

https://doi.org/10.1121/10.0022574

complexity and a slow convergence speed. To overcome such limitation, Akhtar *et al.*[29] proposed an adaptive variable step-size algorithm to accelerate the convergence speed of the identification loop, though the continuous injection of irrelevant signals into the control system will inevitably affect the overall noise control performance of the ANC system as the number of iterations increases. Wang *et al.*[30] introduced a power regulation module to limit the effect of the injection of auxiliary noise on the secondary path identification. The approach involves the injection of a high-power auxiliary signal at the initial stage to accelerate the identification process and gradually reduces the power of the auxiliary signal to mitigate its effect on the control loop and the identification loop at a later stage. Nevertheless, the approach does not solve the problem of system complexity caused by the addition of the auxiliary filter. Alternatively, a simplified identification loop is proposed in this study by modifying the system control loop in addition to the use of the adaptive variable step-size algorithm in the identification process.

II. THE MODELLING OF A SINGLE CHANNEL ANC SYSTEM

A schematic illustration of the proposed single-channel ANC system is shown in Fig. 2 in which the impulse response vectors of the primary path $\mathbf{P}(z)$, secondary path $\mathbf{S}(z)$, and feedback path $\mathbf{F}(z)$ are defined as

$$\mathbf{P}(n) = [p(n), p(n-1), p(n-2), \ldots, p(n-L_p+1)]^T, \quad L_p \in \mathbb{N}, \tag{1a}$$

$$\mathbf{S}(n) = [s(n), s(n-1), s(n-2), \ldots, s(n-L_s+1)]^T, \quad L_S \in \mathbb{N}, \tag{1b}$$

and

$$\mathbf{F}(n) = [f(n), f(n-1), f(n-2), \ldots, f(n-L_f+1)]^T, \quad L_f \in \mathbb{N}, \tag{1c}$$

where T denotes a vector transpose, $\mathbb{N}$ represents positive integers, L_P, L_S, L_f represent the length of the impulse filters.

The primary signal $d(n)$ is described as

$$d(n) = \mathbf{P}^T(n)\mathbf{R}_p(n), \tag{2}$$

where $\mathbf{R}_P(n) = [r(n), r(n-1), r(n-2), \ldots, r(n-L_p+1)]^T$ is the input noise vector, $r(n)$ is the primary noise at the first time instant.

The reference signal $c(n)$ is then

$$c(n) = r(n) + r_f(n), \tag{3}$$

where $r_f(n)$ is the acoustic feedback signal which is given by

$$r_f(n) = \mathbf{F}^T(n)\mathbf{Y}_f(n) \tag{4}$$

and

$$\mathbf{Y}_f(n) = [y_t(n), y_t(n-1), y_t(n-2), \ldots, y_t(n-L_f+1)]^T, \tag{5}$$

where $y_t(n)$ is the sum of the signal output generated by the active control filter.

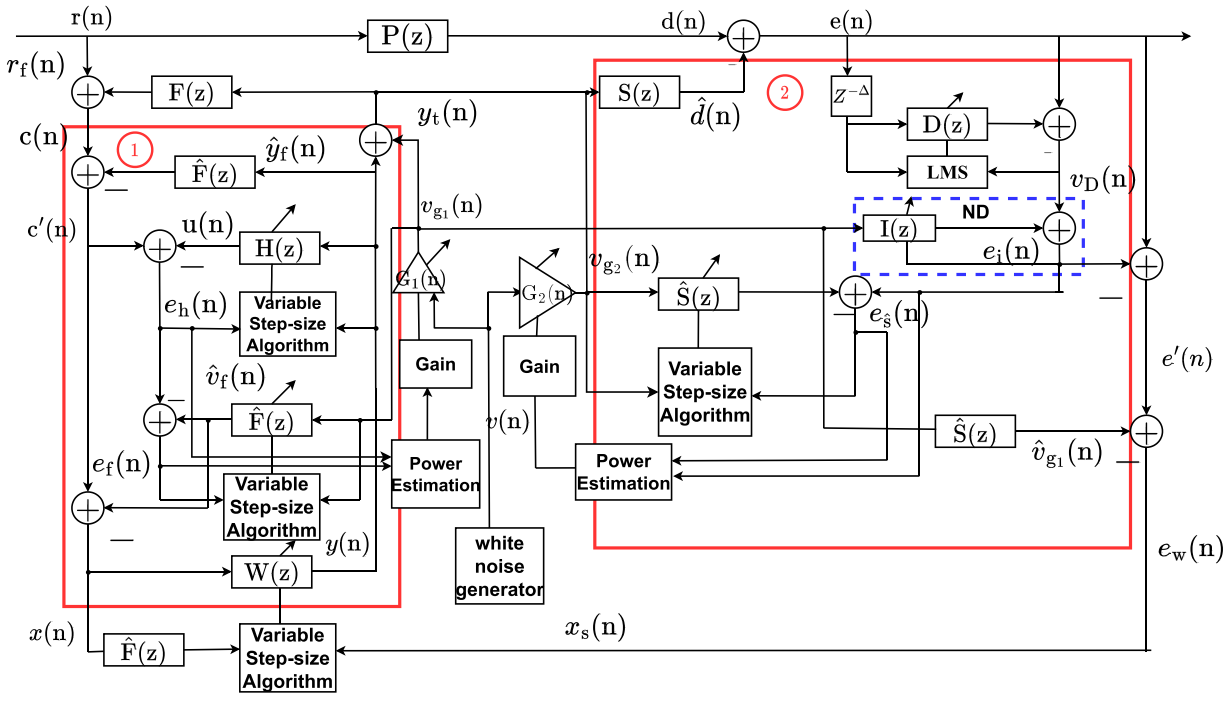

FIG. 2. (Color online) The proposed single channel ANC system.

While the auxiliary noise signal is given by

$$y_t(n) = y(n) + v_{g1}(n), \tag{6}$$

where $v_{g1}(n)$ is the complementary gain signal of the acoustic feedback path defined by

$$v_{g1}(n) = G_1(n)v(n), \tag{7}$$

in which $G_1(n)$ is a variable gain function whose expression will be given in the coming section, $v(n)$ is an added white noise with a unit variance and a zero mean.

When the input signal $r(n)$ and the added white noise $v(n)$ are not correlated, the control error of the ANC system can be expressed by

$$e(n) = d(n) - \hat{d}(n), \tag{8}$$

where $\hat{d}(n) = \mathbf{S}^T(n)\mathbf{Y}_s(n)$, $\mathbf{Y}_s(n) = [y_t(n), y_t(n-1), \ldots, y_t(n-L_s+1)]^T$.

The expression of the control signal from the control loop $y(n)$ is

$$y(n) = \mathbf{W}^T(n)\mathbf{X}_w(n), \tag{9}$$

where $\mathbf{W}(n) = [w_0(n), w_1(n), \ldots, w_{L_w-1}(n)]^T$ are the coefficients of the control filter, and $\mathbf{X}_w(n) = [x(n), x(n-1), \ldots, x(n-L_w+1)]^T$ is the signal entering the control filter.

A virtual path $\hat{\mathbf{F}}(z)$ is proposed in this study to compensate the feedback path of the control loop to address the acoustic feedback problem of the ANC system whose output $\hat{y}_f(n)$ is given by

$$\hat{y}_f(n) = \hat{\mathbf{F}}^T(n)\mathbf{Y}(n), \tag{10}$$

where $\hat{\mathbf{F}}(n) = \left[\hat{f}_0(n), \hat{f}_1(n), \ldots, \hat{f}_{L_f-1}(n)\right]^T$ is the impulse filter of the virtual feedback path, $\mathbf{Y}_d(n) = [y(n), y(n-1), \ldots, y(n-L_f+1)]^T$ is the output vector of the control signal, and the overhead symbol ˆ above the letter represents the virtual loop.

The original auxiliary signal $v(n)$ from the white noise generator will be used to generate the auxiliary signal $v_{g2}(n)$ for the secondary path identification through the gain function $G_2(n)$,

$$v_{g2}(n) = G_2(n)v(n). \tag{11}$$

The definition of the assisted virtual transfer path $\mathbf{H}(z)$ in Fig. 2 will be elaborated on in the following section when the proposed control algorithm is introduced. The major contributions of the proposed algorithm presented in this work are in two folds as highlighted by the two red rectangular windows in Fig. 2, which include the proposition of a virtual acoustic feedback loop to address the interference of the control signal on the reference signal ①, and an optimized secondary path identification loop design ②.

III. THE IDENTIFICATION OF THE ACOUSTIC FEEDBACK AND THE SECONDARY PATH

A. The feedback compensation path

The function of the feedback compensation path is to establish a virtual path, $\hat{\mathbf{F}}(z)$, to simulate the real feedback path $\mathbf{F}(z)$ to eliminate the effect of the real path on the primary noise so that $x(n) \approx r(n)$. A feedback path neutralization (FBPN) filter is usually employed to achieve this purpose by generating an offset feedback signal $\hat{y}_f$(n) as defined by Eq. (10). The FBPN filter is also utilized in this approach to generate a virtual feedback signal to cancel the real feedback signal to minimize the interference of the feedback signal on the stability of the control loop. However, because the original input noise $r(n)$ will also be fed into the FBPN filter in the process, it will slow down the convergence speed of the feedback loop. To address this issue, Kuo and Luan[16] added a predictive filter to the FBPN to filter out the interference of the input noise on the feedback loop for better system convergence. The drawback of their technique is that it requires the original input signal to be predictable which may not be the case in practical applications. As a result, an improved feedback control loop using an adaptive variable step-size noise cancelation filter (ADVSNC) is proposed in this study to overcome this limitation.

For the ADVSNC filter, the filter coefficients $\mathbf{h}$ are updated by

$$\mathbf{h}(n+1) = \mathbf{h}(n) + \mu_h e_h(n)\mathbf{Y}(n). \tag{12}$$

Denoting the desired input signal of the ADVSNC filter as $c'(n)$ and the error output as $e_h(n)$, the following expressions can be obtained:

$$e_h(n) = c'(n) - u(n), \tag{13a}$$

$$c'(n) = r(n) + r_f(n) - \hat{y}_f(n), \tag{13b}$$

$$u(n) = \mathbf{h}^T(n)\mathbf{Y}(n), \tag{13c}$$

where μ_h signifies the convergence factor of the ADVSNC filter, $\mathbf{h}(n) = [h_0(n), h_1(n), \ldots h_{L_h-1}(n)]^T$ is the impulse response of the assisted virtual transfer path $\mathbf{H}(z)$, L_h is the length of $\mathbf{H}(z)$, and $u(n)$ is the output of the control signal $y(n)$ after the ADVSNC filter.

While for the FBPN filter, the filter coefficients are updated using

$$\hat{\mathbf{f}}(n+1) = \hat{\mathbf{f}}(n) + \mu_f\left(e_h(n) - \hat{v}_f(n)\right)\mathbf{v}_{g1}(n), \tag{14}$$

where μ_f is the convergence factor of the FBPN filter, $\hat{\mathbf{f}}(n) = \left[\hat{f}_0(n), \hat{f}_1(n), \ldots, \hat{f}_{L_f-1}(n)\right]^T$ is the impulse response of $\hat{\mathbf{F}}(z)$, L_f is the length of $\hat{\mathbf{F}}(z)$, and $\mathbf{v}_{g1}(n) = [v_{g1}(n), v_{g1}(n-1), v_{g1}(n-2), \ldots, v_{g1}(n-L_f+1)]^T$ is the output vector of the auxiliary noise, $\hat{v}_f(n)$ is the output of the virtual feedback loop.

https://doi.org/10.1121/10.0022574

When $\mathbf{H}(z)$ converges, the output of the ADVSNC filter $u(n)$ will converge to $u(n) \rightarrow r(n) + \big(y(n) * f(n) - \hat{y}_f(n)\big)$, and $e_h(n) \rightarrow v_f(n)$. Thus, the FBPN filter $\hat{\mathbf{F}}(z)$ will receive the desired error signal free of disturbance. When the FBPN filter converges, the error signal will also converge to zero,

$$e_h(n) - \hat{v}_f(n) = 0, \tag{15}$$

so that $v_f(n) \approx \hat{v}_f(n)$, $\mathbf{F}(z) \approx \hat{\mathbf{F}}(z)$, $y(n) * f(n) \approx \hat{y}_f(n)$.

The input signal to the controller can now be written as

$$x(n) = r(n) + \mathrm{y}(n) * f(\mathrm{n}) - \hat{v}_f(n) - \hat{y}_f(n) + v_f(n). \tag{16}$$

According to Eq. (16), when both ADVSNC and FBPN filters converge, the input signal of the controller can be a good approximation of the noise signal such that $x(n) \approx r(n)$. The advantage of the proposed approach in comparison to the acoustic feedback design by Aslam *et al.*[18] is that it can produce a closely matched input signal to the controller without prior knowledge of the original noise signal. Furthermore, their algorithm overly relies on the linear predictive filter, if the delay of the predictive filter is not handled well, it can cause the control system to diverge. The system instability problem associated with the use of linear predictive filters can be effectively avoided by using the proposed approach enclosed by the red rectangular window ① in Fig. 2.

B. The secondary path identification

A least mean square (LMS) filter is added to the output of the residual signal $e(n)$, in which the delay Δ is used to ensure the decorrelation of the auxiliary noise $v_{g2}(n)$ used by the FBPN filter $\hat{\mathbf{F}}(z)$, while the narrowband components from the LMS filter remain correlated to external interference. A detailed derivation of the correlation function between the error signals $e(n)$ and $e(n-\Delta)$ of the LMS filter is presented in Appendix A, whereas the formula is given as follows:

$$\begin{aligned} \mathrm{E}\big[e(n)e(n-\Delta)\big] = {} & \mathrm{E}\big[k(n)k(n-\Delta)\big] \\ & + \sum_{i=0}^{L_s-1} s_i(n) \sum_{j=0}^{L_s-1} s_j(n) \\ & \times \mathrm{E}\big[v(n-i)v(n-j-\Delta)\big], \end{aligned} \tag{17}$$

in which E represents the mathematic expectation, * denotes the linear convolution, L_s is the length of the secondary path $\mathbf{S}(z)$, $k(n) = d(n) + s(n) * y(n)$ is the interference of the primary path on the LMS filter, $v(n) = v_{g1}(n) + v_{g2}(n)$. Because $v_{g2}(n)$ is a white noise signal with zero mean, so when $\Delta \geq L_s$, the last term of Eq. (17) becomes zero,

$$\mathrm{E}\big[v(n-i)v(n-j-\Delta)\big] = 0, \quad for \ i < L_s, j \geq 0. \tag{18}$$

When $\Delta \geq L_s$, the correlation components in $e(n)$ and $e(n-\Delta)$ will be filtered out as the coefficients of the LMS filter $\mathbf{D}(z)$ which are continuously updated until they converge. While the uncorrelated component $v(n)$ will be fed into the secondary path identification as the desired signal indicating that there will be no interference from the primary path in the secondary path identification. However, if $\Delta < L_s$, the second term in Eq. (17) will not be zero, which will cause the training component $k(n)$ to pass through $\mathbf{D}(z)$, thus affecting the convergence of $\hat{\mathbf{S}}(z)$. Since $v(n)$ also contains the auxiliary increment $v_{g1}(n)$ from the acoustic feedback, the $v(n)$ obtained from the LMS filter $\mathbf{D}(z)$ cannot be directly used in the secondary path identification. An additional noise decoupling (ND) filter is thus designed in this study (enclosed by the dashed blue rectangle in Fig. 2) to remove the noise component $v_{g1}(n)$.

Defining the output of the signal component $v_{g1}(n)$ after the ND filter as

$$v_{g_{1i}}(n) = \mathbf{v}_{g1}(n) * \mathbf{I}(n) \tag{19}$$

and

$$\mathbf{I}(n+1) = \mathbf{I}(n) + \mu_I \big(v_D(n) - v_{g_{1i}}(n)\big)\mathbf{v}_{g1}(n), \tag{20}$$

where $\mathbf{I}(n) = [i_0(n), i_1(n), \ldots, i_{L_i-1}(n)]^T$ are the impulse response of the assisted virtual transfer path $\mathbf{I}(z)$, μ_I is the convergence factor, L_i is the length, and $v_D(n)$ is the output of the LMS filter. Since the signal component $v_{g1}(n)$ is mixed in $v(n)$, the error output of the ND filter will gradually converge to $[v_{g2}(n) * s(n)]$, which can ensure that there are no irrelevant interference terms in the subsequent secondary path identification. Moreover, because the control error signal in traditional secondary path identification is used directly as the error of the control filter, it can lead to system instability as the error signal also contains auxiliary noise components from the secondary path. Aiming to alleviate this problem, this study presents an alternative second path identification loop design as enclosed by the red rectangular window ② in Fig. 2 to remove the interference from the auxiliary noise in the control signal.

Giving the error signal entering the control filter as

$$e_w(n) = e(n) - \big(v_D(n) - v_{g_{1i}}(n)\big) - \hat{v}_{g1}(n), \tag{21}$$

where $\hat{v}_{g1}(n) = v_{g1}(n) * \hat{s}(n)$, when the system converges, $\big(v_D(n) - v_{g_{1i}}(n)\big) \rightarrow v_{g2}(n) * s(n)$, thus we have

$$e_w(n) \approx d(n) + \hat{y}_s(n), \tag{22}$$

where $\hat{y}_s(n) = y(n) * s(n)$.

IV. A DERIVATION OF THE ADAPTIVE ALGORITHM

A. An adaptive algorithm for the virtual feedback loop $\hat{\mathbf{F}}(z)$

In this subsection, a detailed derivation of the adaptive variable step-size algorithm is presented. The input reference signal $c(n)$ entering the control loop enclosed by the red rectangular window ① in Fig. 2 can be written as

$$c(n) = \mathbf{f}^T(n)\mathbf{v}_{g1}(n) + v_{xx}(n) \tag{23}$$

and

$$v_{xx}(n) = r(n) + \mathbf{f}^T(n)\mathbf{Y}(n), \tag{24}$$

where $v_{xx}(n)$ is the interference to the virtual path $\hat{\mathbf{F}}(z)$.

The prior and posterior errors of the feedback compensation FBPN filter $\hat{\mathbf{f}}(n)$ are defined as

$$e_f(n) = \mathbf{v}_{g1}^T(n)\left[\mathbf{f}(n) - \hat{\mathbf{f}}(n)\right] + v_x(n), \tag{25}$$

$$\varepsilon_f(n) = \mathbf{v}_{g1}^T(n)\left[\mathbf{f}(n) - \hat{\mathbf{f}}(n+1)\right] + v_x(n), \tag{26}$$

and

$$v_x(n) = v_{xx}(n) - \mathbf{h}^T(n)\mathbf{Y}(n), \tag{27}$$

where $\hat{\mathbf{f}}(n)$ and $\hat{\mathbf{f}}(n+1)$ are the estimates of the virtual acoustic feedback path $\hat{\mathbf{F}}(z)$ at time n and $n+1$.

Whereas the linear update variance of $\hat{\mathbf{f}}(n+1)$ is

$$\hat{\mathbf{f}}(n+1) = \hat{\mathbf{f}}(n) + \mu_f(n)\mathbf{v}_{g1}(n)e_f(n), \tag{28}$$

where $\mu_f(n)$ is the convergence factor of the update function, $e_f(n)$ is the output error of the FBPN filter.

Substituting Eq. (28) into Eq. (26), and using the Lagrange multiplier for normalization,[31] we have

$$\mu_f(n) = \frac{\mathrm{E}\{e_f{}^2(n)\} - \mathrm{E}\{v_x{}^2(n)\}}{\|v_{g1}(n)\|\mathrm{E}\{e_f{}^2(n)\}}. \tag{29}$$

According to Eq. (29), the convergence factor converges to a fixed value $\mu_f(n) = \left[\mathbf{v}_{g1}^T(n)\mathbf{v}_{g1}(n)\right]^{-1}$ when the interference signal $v_x(n)$ disappears and $e_f(n) \neq 0$.[31] However, the normalization becomes meaningless when the virtual path contains the interference signal because $\mathbf{v}_{g1}^T(n)\left[\mathbf{f}(n) - \hat{\mathbf{f}}(n+1)\right] = -v_x(n) \neq 0$. To resolve this issue, we need to let the first term on the righthand side of Eq. (26), $\mathbf{v}_{g1}^T(n)\left[\mathbf{f}(n) - \hat{\mathbf{f}}(n+1)\right] = 0$, $n \in \mathbb{R}$, which implies $\varepsilon_f = v_x(n)$. This can be achieved by letting the expectation of the power error $\varepsilon_f^2(n)$ equals to the power of the standard deviation of $v_x(n)$.

The estimate error $\varepsilon_f(n)$ can be obtained from Eqs. (25), (26), and (28) as

$$\varepsilon_f(n) = \left[1 - \mu_f(n)\mathbf{v}_{g1}^T(n)\mathbf{v}_{g1}(n)\right]e_f(n). \tag{30}$$

The power output of the auxiliary noise vector $\mathbf{v}_{g1}(n)$ can be approximated by

$$\mathbf{v}_{g1}^T(n)\mathbf{v}_{g1}(n) = L_f\sigma_{v_{g1}}^2 \quad \text{for} \quad L_f \gg 1. \tag{31}$$

From Eqs. (30) and (31), the expectation of the power error $\varepsilon_f^2(n)$, $\mathrm{E}\left[\varepsilon_f^2(n)\right]$ can be obtained as

$$\begin{aligned}\mathrm{E}\left[\varepsilon_f^2(n)\right] &= \left[1 - \mu_f(n)L_f\mathbf{v}_{g1}^T(n)\mathbf{v}_{g1}(n)\right]^2\sigma_{e_f}^2(n)\\ &= \left[1 - \mu_f(n)L_f\sigma_{v_{g1}}^2\right]^2\sigma_{e_f}^2(n)\\ &= \sigma_{v_x}^2.\end{aligned} \tag{32}$$

From Eq. (32), the following linear equation can be obtained:

$$\mu_f{}^2(n) - \frac{2}{L_f\sigma_{v_{g1}}^2}\mu_f(n) + \frac{1}{\left(L_f\sigma_{v_{g1}}^2\right)^2}\left[1 - \frac{\sigma_{v_x}^2}{\sigma_{e_f}^2(n)}\right] = 0, \tag{33}$$

which renders a positive root for the convergence factor,

$$\mu_f(n) = \frac{1}{\mathbf{v}_{g1}^T(n)\mathbf{v}_{g1}(n)}\left[1 - \frac{\sigma_{v_x}}{\sigma_{e_f}(n)}\right], \tag{34a}$$

or

$$\mu_f(n) = \frac{1}{L_f\sigma_{v_{g1}}^2}\alpha_f(n), \quad \alpha_f(n) \in [0, 1]. \tag{34b}$$

Substituting Eq. (34b) into Eq. (28) to have

$$\hat{\mathbf{f}}(n+1) = \hat{\mathbf{f}}(n) + \frac{\alpha_f(n)}{L_f\sigma_{v_{g1}}^2}\mathbf{v}_{g1}(n)e_f(n). \tag{35}$$

According to Eq. (34a), the convergence factor will take a small incremental value at the early stage of the iteration since $\sigma_{e_f}(n) > \sigma_{v_x}(n)$, in which the system converges slowly, whereas the convergence factor will take a large incremental value at the later convergence stage as $\sigma_{v_x} \approx \sigma_{e_f}(n)$ so the system will converge at a faster speed.

To prevent the system instability caused by a small denominator $\sigma_{ef}(n)$ in Eq. (34a), a random small value k is introduced into Eq. (35) to be in the form

$$\begin{aligned}\hat{\mathbf{f}}(n+1) = \hat{\mathbf{f}}(n) + \left(k + \frac{\alpha_f(n)}{L_f\sigma_{v_{g1}}^2}\right)\mathbf{v}_{g1}(n)e_f(n)\\ \text{for} \quad k \in \forall[0,\ 0.05],\end{aligned} \tag{36}$$

where $\alpha_f(n)$ is re-defined by including an adaptive adjustment factor $\sqrt{\sigma_{v_x}^2(n)/\sigma_{v_{g1}}^2(n)}$ as

$$\alpha_f(n) = 1 - \frac{\sigma_{v_x}}{\sqrt{\frac{\sigma_{v_x}^2(n)}{\sigma_{v_{g1}}^2(n)}} + \sigma_{e_f}(n)} \tag{37a}$$

and

$$\alpha_f = \begin{cases} 0, & \alpha_f < 0,\\ \alpha_f & \text{other}, \end{cases} \tag{37b}$$

in which $\sigma_{v_x}^2(n)$ will gradually decrease to 0 as the number of iterations increases to ensure the system convergence and stability.

https://doi.org/10.1121/10.0022574

The standard deviations of the error signal, the auxiliary signal, and the interference signal of the FBPN filter, $\sigma^2_{e_f}(n)$, $\sigma^2_{v_{g1}}(n)$, $\sigma^2_{v_x}(n)$, can now be evaluated using the exponential recursive weight algorithm[31]

$$\sigma^2_{e_f}(n+1) = \beta\sigma^2_{e_f}(n) + (1-\beta)e^2_f(n+1), \tag{38}$$

$$\sigma^2_{v_{g1}}(n+1) = \beta\sigma^2_{v_{g1}}(n) + (1-\beta)v^2_{g1}(n+1), \tag{39}$$

and

$$\sigma^2_{v_x}(n+1) = \beta\sigma^2_{v_x}(n) + (1-\beta)v^2_x(n+1), \tag{40}$$

where β refers to a forgetting factor that assumes a random value between 0.9 and 1.

B. An adaptive algorithm for the assisted transfer path H(z) in the acoustic feedback loop

The adaptive algorithm derived in Sec. IV A for the FBPN filter can also be applied to the ADVSNC filter in the assisted transfer path $\mathbf{H}(z)$. Accordingly, the error signal $e_h(n)$ in Eq. (12) can be re-expressed in terms of the desired input signal and the convergence factor of the ADVSNC filter as

$$\begin{aligned} e_h(n) &= t'(n) - u(n) \\ &= \big(r(n) + y_f(n) - \hat{y}_f(n)\big) \\ &\quad + \big(v_{g1}(n) * f(n) - y(n) * h(n)\big), \end{aligned} \tag{41a}$$

which can be simplified into two signal components,

$$e_h(n) = v_{disturb} + v_{useful}. \tag{41b}$$

From Eq. (12), the convergence factor of the ADVSNC filter can now be written as

$$\mu_h(n) = \frac{1}{\mathbf{Y}^T(n)\mathbf{Y}(n)}\left[1 - \frac{\sigma_{v_{disturb}}}{\sigma_{e_h}(n)}\right] = \frac{1}{L_h\sigma^2_y}\alpha_h(n). \tag{42}$$

The coefficient iterative equation of the ADVSNC filter can be written in a similar form of Eq. (36),

$$\mathbf{h}(n+1) = \mathbf{h}(n) + \left(k + \frac{\alpha_h(n)}{L_h\sigma^2_y}\right)\mathbf{Y}(n)e_h(n) \quad \text{for} \quad k \in \forall[0,\ 0.05]. \tag{43}$$

The rest of the algorithm are the same as those described in Sec. IV A by simply interchanging the corresponding variables in Eqs. (37)–(40). The same algorithm can also be applied to the filters of the virtual secondary path $\hat{\mathbf{S}}(z)$ and the system controller transfer path $\mathbf{W}(z)$, which derivation will not be repeated here to be concise.

V. THE DESIGN OF AN AUXILIARY SIGNAL GAIN

A. The gain of the acoustic feedback path

Auxiliary signals are needed in the acoustic feedback path (enclosed by the red rectangular window ① in Fig. 2) and the secondary path (window ② in Fig. 2) in the proposed control system for compensation and identification. Therefore, two different gain functions are defined for these two loops. The gain $G_1(n)$ for the acoustic feedback path is derived in this subsection.

Defining the power of the control output signal $y(n)$ and the auxiliary signal $v_{g1}(n)$ through the acoustic feedback path $\mathbf{F}(z)$ as $P_{y_f}(n)$, $P_{v_f}(n)$, the power of the error output signal $e_h(n)$ of the ADVSNC filter, $P_{e_h}(n)$, can be expressed as

$$P_{e_h}(n) = P_{(y_f+v_f)}(n) - P_{y_f}(n). \tag{44a}$$

Equation (44a) can be expanded by[31]

$$\begin{aligned} P_{e_h}(n) &= \|f(n)\|^2\Big[\mathrm{E}[y_f(n)^2] + G_1^2(n)\mathrm{E}[v(n)^2]\Big] \\ &\quad - \|f(n)\|^2\mathrm{E}\Big[y_f(n)^2\Big], \end{aligned} \tag{44b}$$

where $\|\cdot\|$ represents the squared Euclidean norm, $y_f(n) = \mathbf{f}^T(n)\mathbf{Y}(n)$.

It can be seen from Eq. (7) that the added noise $v(n)$ is a white noise with zero mean value and unit variance, so the average power of $v(n)$ is unity. As a result, Eq. (44b) can be simplified by extracting the common terms to be in the following form:

$$P_{e_h}(n) = G_1^2(n)\|f(n)\|^2. \tag{44c}$$

From Eq. (44c), the gain of the acoustic feedback path can be obtained,

$$G_1(n) = \sqrt{\frac{P_{e_h}(n)}{\|f(n)\|^2}}. \tag{45}$$

The updating equation for the power of the error output signal $P_{e_h}(n)$ can once again be evaluated using the exponential recursive weighting algorithm[31]

$$P_{e_h}(n+1) = \lambda P_{e_h}(n) + (1-\lambda)e^2_h(n+1) \quad \text{for } \lambda \in [0.9,\ 1], \tag{46}$$

where λ refers to a forgetting factor which assumes a random value between 0.9 and 1.

From Eqs. (45) and (46), it can be found that at the initial stage where $\mathbf{H}(z)$ has not yet converged, the gain of the filter, $G_1(n)$, is large since the input error $e_h(n)$ is large. Therefore, it will force the filter to converge at a faster speed. After several iterations, $e_h(n)$ will gradually converge to a smaller and stable value, so is the gain is $G_1(n)$, thus leading to the injection of a smaller auxiliary noise into the ADVSNC filter. The gain $G_2(n)$ used in the secondary path identification can also be designed in a similar manner, which will not be repeated here.

VI. CONVERGENCE OF THE MISALIGNMENT BETWEEN THE VIRTUAL AND THE REAL ACOUSTIC FEEDBACK PATHS

This section analyzes the convergence of the output signals between the virtual and the real acoustic feedback paths

based on an independence assumption.[32] Note that the process presented here can also be used in the analysis of the secondary path identification which will not be elaborated on in this study.

Two main assumptions are made in the analysis:

(1) The output vector of the auxiliary noise $\mathbf{v}_{g1}(1), \mathbf{v}_{g1}(2), \ldots, \mathbf{v}_{g1}(n)$ are statistically independent where n denotes the sequential index of iterations.
(2) At the nth iteration, the desired output of $\mathbf{F}(z)$ depends on $\mathbf{v}_{g1}(n)$. The current desired output of $\mathbf{F}(z)$ and $\mathbf{v}_{g1}(n)$ are statistically independent of all past outputs of $\mathbf{F}(z)$.

The misalignment vector is defined as

$$\mathbf{m}_f(n) = \mathbf{f}(n) - \hat{\mathbf{f}}(n). \tag{47}$$

To simplify the calculation of the misalignment, let the bracket term in Eq. (36) be

$$\left(k + \frac{\alpha_f(n)}{L_f \sigma^2_{v_{g1}}}\right) = \gamma \frac{\alpha_f(n)}{L_f \sigma^2_{v_{g1}}}, \tag{48}$$

where $\gamma = 1 + k/\alpha_f(n)/L_f\sigma^2_{vg1}$. Equation (36) can now be re-expressed as

$$\hat{\mathbf{f}}(n+1) = \hat{\mathbf{f}}(n) - \gamma \frac{\alpha_f(n)}{L_f \sigma^2_{v_{g1}}} \mathbf{v}_{g1}(n) e_f(n). \tag{49}$$

Substituting Eq. (49) into Eq. (47), the misalignment between the virtual and the real acoustic feedback paths can be written as

$$\mathbf{m}_f(n) = \mathbf{m}_f(n-1) - \gamma \frac{\alpha_f(n-1)}{L_f \sigma^2_{v_{g1}}} \mathbf{v}_{g1}(n-1) e_f(n-1). \tag{50}$$

Taking the norms on both sides of Eq. (50), the mathematic expectation for the misalignment can be obtained,

$$\begin{aligned} E\left[\|\mathbf{m}_f(n)\|_2^2\right] &= E\left[\|\mathbf{m}_f(n-1)\|_2^2\right] - 2\gamma \frac{\alpha_f(n-1)}{L_f \sigma^2_{v_{g1}}} \\ &\quad \times \mathrm{E}\left[\mathbf{v}^T_{g1}(n-1)\mathbf{m}_f(n-1)e_f(n-1)\right] \\ &\quad + \gamma^2 \frac{\alpha_f^2(n-1)}{L_f^2 \sigma^4_{v_{g1}}} E\left[e_f^2(n-1)\right. \\ &\quad \left. \times \mathbf{v}^T_{g1}(n-1)\mathbf{v}_{g1}(n-1)\right]. \end{aligned} \tag{51}$$

A detailed derivation of Eq. (51) is given in Appendix B for interested readers. From Eq. (51), we have

$$\begin{aligned} E\left[\|\mathbf{m}_f(n)\|_2^2\right] &= g\left(\alpha_f(n-1), L_f\right) \\ &\quad \times \mathrm{E}\left[\|\mathbf{m}_f(n-1)\|_2^2\right] \\ &\quad + b\left(\alpha_f(n-1), L_f, \sigma^2_{v_{g1}}, \sigma^2_{v_x}, \gamma\right), \end{aligned} \tag{52a}$$

where the misalignment rate is

$$\begin{aligned} g\left(\alpha_f(n-1), L_f\right) &= 1 - 2\frac{\alpha_f(n-1)}{L_f} \\ &\quad + \frac{(L_f+2)\alpha_f^2(n-1)}{{L_f}^2}, \end{aligned} \tag{52b}$$

and the misalignment amount is

$$b\left(\alpha_f(n-1), L_f, \sigma^2_{v_{g1}}, \sigma^2_{v_x}, \gamma\right) = \frac{\alpha_f^2(n-1)\gamma^2}{L_f \sigma^2_{v_{g1}}} \sigma^2_{v_x}. \tag{52c}$$

During the fast convergence stage of the FBPN filter, the incremental increase in the misalignment rate $g\left(\alpha_f(n-1), L_f\right)$ takes a small step. The value of the incremental can be determined by taking the derivative of Eq. (52b) with respect to α_f and letting it equal zero,

$$\alpha_f(n-1) = \frac{L_f}{L_f + 2}. \tag{53}$$

When the system becomes stable, $\mathrm{E}\left[\|\mathbf{m}_f(n)\|_2^2\right]$ will gradually converge, this means $g\left(\alpha_f(n-1), L_f\right) \to 1$, and

$$\alpha_f(n-1) \to \frac{2L_f}{L_f + 2}. \tag{54}$$

From Eq. (52c), it can be seen when $\alpha_f(n)$ increases, the misalignment amount between the virtual and the real acoustic feedback paths increases, and vice versa. The minimum misalignment occurs when $\alpha_f(n) \approx 0$. That is, when $\sigma_{v_x} = \sqrt{[\sigma^2_{v_x}(n-1)]/[\sigma^2_{v_{g1}}(n-1)]} + \sigma_{e_f}(n-1)$, The stability of the system and the accuracy of the acoustic feedback path compensation will also be the highest. With the increased number of iterations, the adjustment factor $\sqrt{[\sigma^2_{v_x}(n-1)]/[\sigma^2_{v_{g1}}(n-1)]}$ decreases gradually, and $\sigma_{v_x}(n-1) \approx \sigma_{e_f}(n-1)$ when the iteration terminated.

VII. CASE STUDIES

A. Case 1

The advantage of the proposed control algorithm is evaluated by the control performance of an input noise signal containing multiple low frequency tonal components, and the noise reduction result is compared to that using only an improved acoustic feedback loop[18] and that using only a secondary path loop.[24,25,34]

The simulated input noise signal used in this case study is a mixture of three sinusoidal tonal components at 100, 200, 300 Hz as described by

$$\begin{aligned} r(t) &= 0.4\sin(2\pi{*}100t) + 0.8\sin(2\pi * 200t) \\ &\quad + \sin(2\pi{*}300t) + \mathrm{wgn}, \end{aligned} \tag{55}$$

where t denotes the time, wgn represents a random white Gaussian noise with signal-to-noise ratio (SNR) $= -3$ dB.

https://doi.org/10.1121/10.0022574

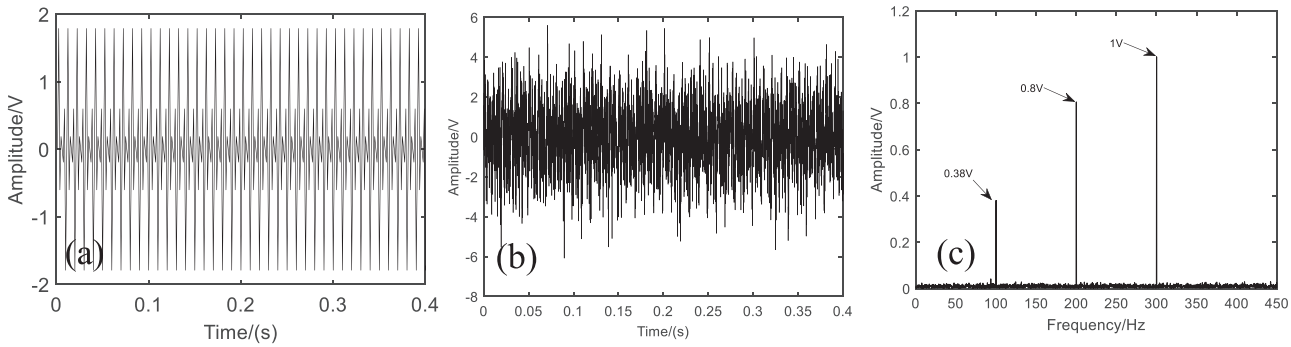

FIG. 3. The simulated input noise signal $r(t)$, (a) the pure tone signal, (b) the noise added signal (SNR=-3dB), and (c) the frequency spectrum.

The time waveform and the frequency spectrum of the simulated signal is shown in Fig. 3.

In order to verify the accuracy of the acoustic feedback path compensation and the secondary path identification, the following formulas are used to evaluate the relative compensation error and relative identification error:

$$\Delta F(n) = 10\log_{10}\left(\frac{\|\mathbf{f}(n)-\hat{\mathbf{f}}(n)\|^2}{\|\mathbf{f}(n)\|^2}\right) \tag{56}$$

and

$$\Delta S(n) = 10\log_{10}\left(\frac{\|\mathbf{s}(n)-\hat{\mathbf{s}}(n)\|^2}{\|\mathbf{s}(n)\|^2}\right), \tag{57}$$

where $\Delta F(n)$ is the relative compensation error of the acoustic feedback path, and $\Delta S(n)$ is the relative identification error.

The calculated relative compensation error of the acoustic feedback path using the proposed technique and that of Aslam *et al.*[18] as a function of the number of iterations are compared in Fig. 4. It is shown that the proposed algorithm renders a smaller relative compensation error than that of Aslam *et al.*[18] in addition to a much faster convergence speed. This is because the algorithm proposed by Aslam *et al.*[18] needs to deal with the delay caused by the linear prediction filter leading to a slower convergence of the loop. Furthermore, because an adaptive adjustment weight factor $\sqrt{\sigma^2_{v_x}(n)/\sigma^2_{v_{g1}}(n)}$ was introduced in the proposed algorithm, it can increase the compensation accuracy.

The calculated relative identification error of the secondary path using the proposed technique and those of Eriksson and Allie,[24] Zhang and Lan,[25] Dong *et al.*[34] are compared in Fig. 5. It is shown that the proposed algorithm has the smallest relative identification error within all algorithms. The reason the algorithms proposed by Dong *et al.*[34] and Zhang and Lan[25] are not as accurate as that of the proposed technique is that they do not consider the interference of the acoustic feedback path on the second path identification. Whereas the relative identification error produced by the Eriksson and Allie algorithm[24] implies that the algorithm cannot meet the identification requirement and the system is diverged due to a lack of the acoustic feedback path on the secondary path and the interference between the active control filter $\mathbf{W}(z)$ and the secondary path identification filter $\mathbf{S}(z)$ in the system.

Figure 6 shows the spectrograms of the input noise signal and the control output error signal using the proposed algorithm and those of Dong *et al.*,[34] Zhang and Lan,[25] and

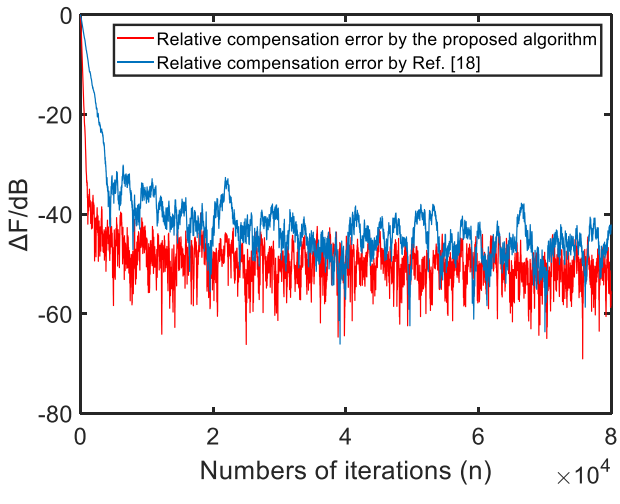

FIG. 4. (Color online) Acoustic feedback path compensation error.

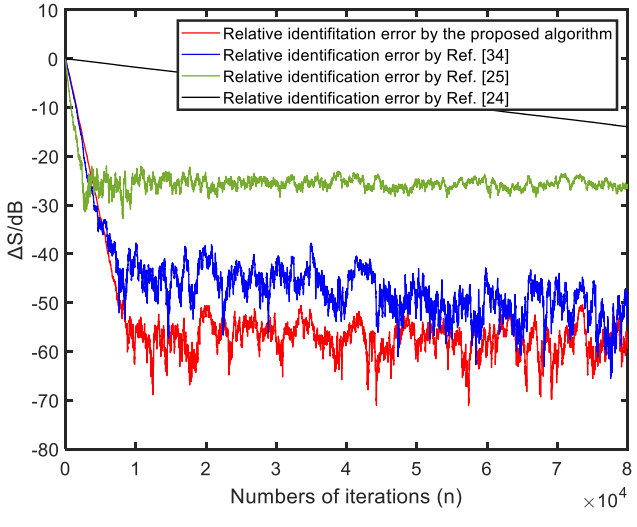

FIG. 5. (Color online) Secondary path identification error.

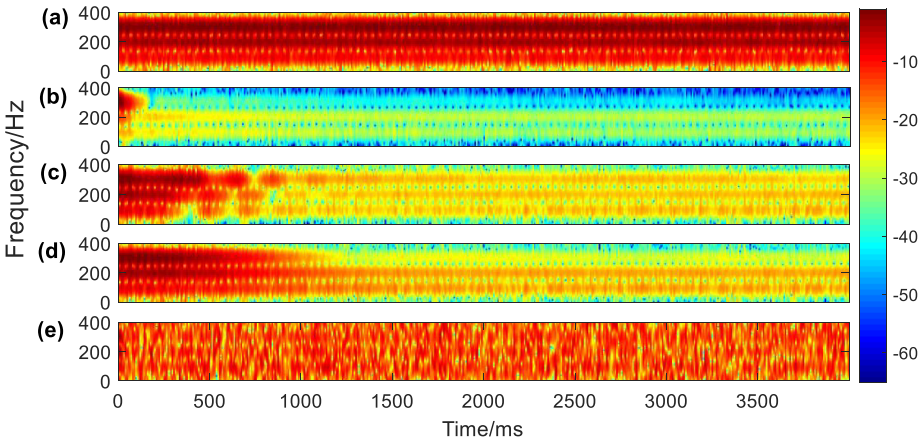

FIG. 6. (Color online) The spectrograms of the input and output signals, (a) the input noise signal, (b) the output of the proposed ANC system, (c) the output of the Dong *et al.* (Ref. 34) system, (d) the output of the Zhang and Lan (Ref. 25) system, and (e) the output of the Eriksson and Allie (Ref. 24) system.

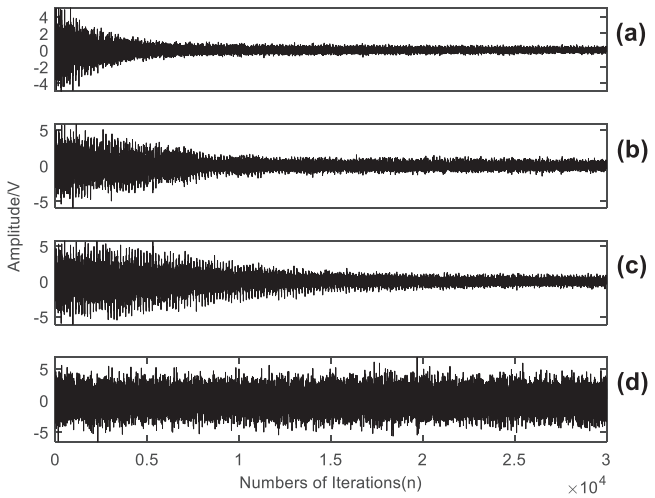

FIG. 7. The amplitude of the residual error signal $e(n)$ versus the number of iterations, (a) the proposed algorithm, (b) the Dong *et al.* algorithm (Ref. 34). (c) Zhang & Lan's algorithm (Ref. 25), and (d) Eriksson & Allie's algorithm (Ref. 24).

Eriksson and Allie.[24] It is shown in Fig. 6 that the signal energies of the three major frequency components at 100, 200, and 300 Hz using the proposed control algorithm are quickly reduced to a small level after less than 0.1 s. While the algorithm proposed by Dong *et al.*[34] takes a much longer time (around 0.8 s) to converge in addition to a higher level of residual noise. It takes about 1.3 s for the system to converge using the Zhang and Lan[25] algorithm, where the system performance on the noise reduction for the two low frequency components at 100 and 200 Hz is rather poor. Whereas the Eriksson and Allie[24] ANC system yields a diverged control outcome due to the inability of the system to accurately identify the secondary path.

Figure 7 compares the convergence speed of the proposed algorithm and those of the other three algorithms as a function of the number of iterations. It is shown that the converging speed of the system to a steady state using the proposed algorithm is at least twice faster than the other algorithms, and the amplitude of the error signal is very small.

Figure 8 compares the sound pressure spectra of the input noise signal and the output error signals using the proposed algorithm and the other three algorithms. It is shown

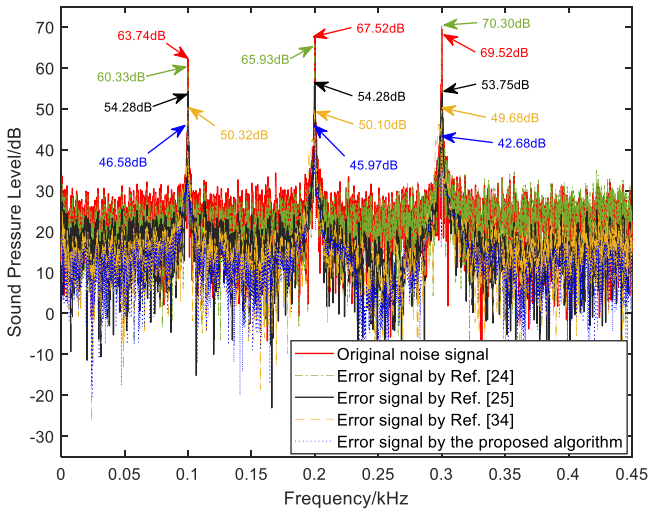

FIG. 8. (Color online) A comparison of the noise control performance using various algorithms.

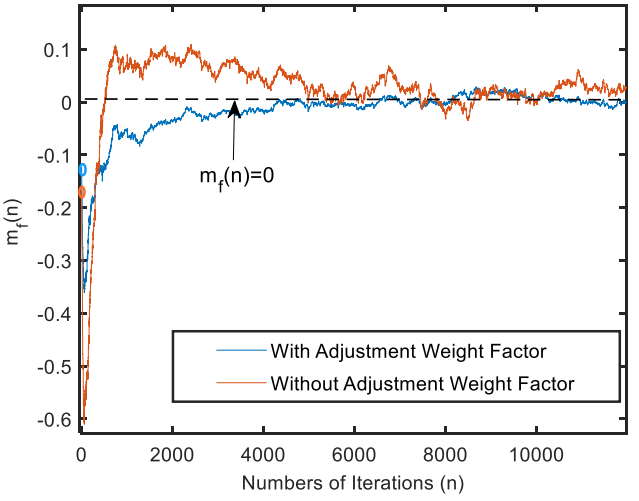

FIG. 9. (Color online) Convergence of the misalignment of the acoustic feedback paths and compare the effect of adjusting weighting factor on the convergence of the misalignment. Note the ellipses in the figure indicate where the iteration begins.

https://doi.org/10.1121/10.0022574

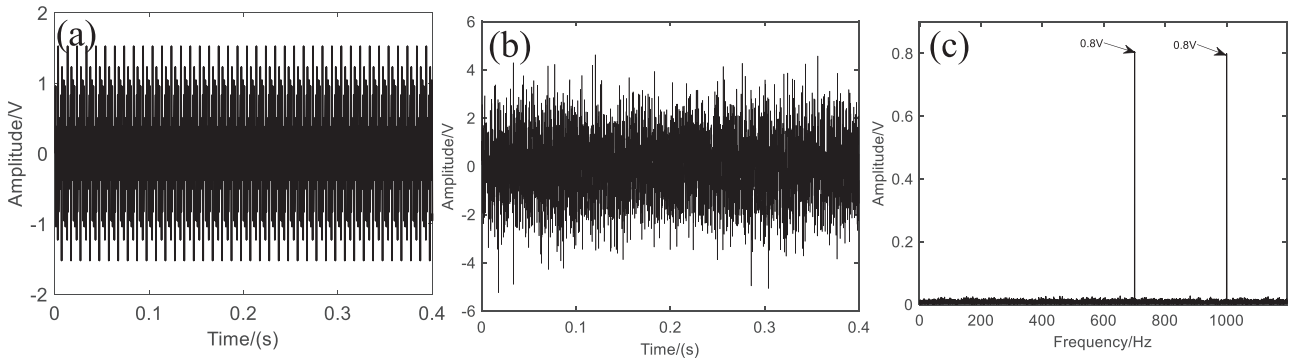

FIG. 10. The simulated input noise signal $r(t)$, (a) the time waveform, (b) the noise added signal (SNR = −3 dB), and (c) the frequency spectrum.

that the original sound pressure levels (63.74, 67.52, and 69.52 dB) of the noise components at 100, 200, and 300 Hz have been successfully reduced to 46.58, 45.97, and 42.68 dB using the proposed algorithm. The control outcome using the Dong *et al.*[34] and Zhang and Lan[25] algorithms is not as good, whereas there is almost no reduction on the three noise components using the Eriksson and Allie[24] algorithm. The result indicates that the proposed algorithm has a superior performance on the low frequency noise control of multi-component input signals.

Figure 9 compares the convergence of the misalignment $\mathbf{m}_f(n)$ as a function of the number of iterations with and without the adjustment weight factor in the variable step-size algorithm. It is shown that when the iteration starts, the misalignment will have a large fluctuation in a very short interval (about 100 iterations), and converges quickly toward zero after 2000 iterations when the adjustment weight factor is used. On the other hand, the convergence curve of the misalignment $\mathbf{m}_f(n)$ has an even larger fluctuation when the adjustment weight factor is not included in the algorithm.

B. Case 2

To further evaluate the effectiveness of the proposed algorithm, a mid-frequency noise with two sinusoidal tonal components at 700 and 1000 Hz as described below are simulated and used as the input noise signal to test the control performance of the algorithm,

$$r(t) = 0.8\sin(2\pi*(700t+\phi)) + 0.8\sin(2\pi*(1000t+\phi)) + \text{wgn}, \quad (58)$$

where ϕ represents a random phase having a value between 1 and 10, and wgn is an added random white Gaussian noise with SNR = −3 dB. The time waveform and the frequency spectrum of the simulated input noise signal are shown in Fig. 10.

The simulated signal is fed into the proposed active control system with a virtual acoustic feedback loop and an optimized secondary path identification loop shown in Fig. 2. The calculated frequency response of the virtual acoustic feedback loop $\hat{\mathbf{F}}_1(z)$ is shown in Fig. 11(a). Also, shown in the figure are the frequency response of the real acoustic feedback path $\mathbf{F}(z)$ and that calculated using the algorithm presented by Aslam *et al.*[18] [$\hat{\mathbf{F}}_2(z)$] for comparison. It is shown that the algorithm presented in this work can yield a closely matched frequency response to that of the real feedback path so that the influence of the acoustic feedback path can be canceled, leading to a good noise cancellation result of the ANC system. On the other hand, it is shown that the

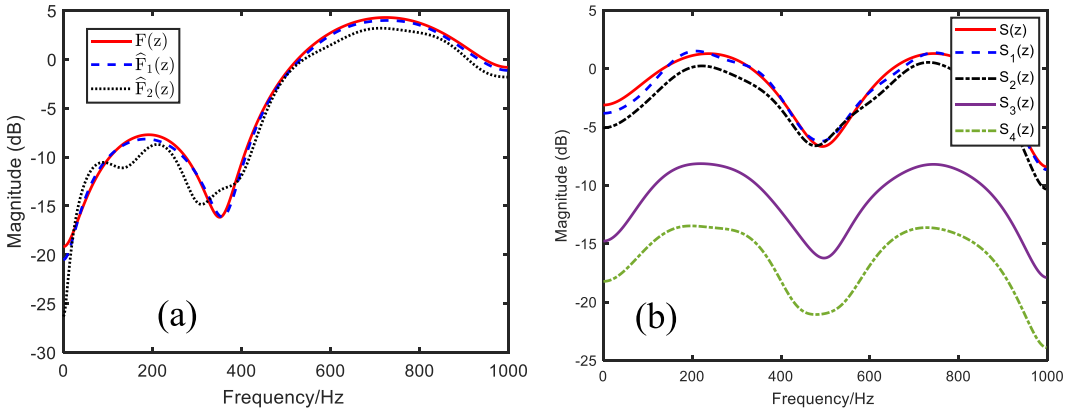

FIG. 11. (Color online) The frequency response curves, (a) the acoustic feedback path, (b) the secondary path. Note: $\mathrm{F}(z)$, $\hat{\mathrm{F}}_1(z)$, $\hat{\mathrm{F}}_2(z)$ represent the real acoustic feedback path and the virtual acoustic feedback path calculated by the proposed algorithm and the Aslam *et al.* algorithm (Ref. 18), respectively. While $\mathrm{S}(z)$, $\hat{\mathrm{S}}_1(z)$, $\hat{\mathrm{S}}_2(z)$, $\hat{\mathrm{S}}_3(z)$, $\hat{\mathrm{S}}_4(z)$ represent the secondary path, and the virtual secondary path calculated by the proposed algorithm, the Dong *et al.* algorithm (Ref. 34), Zhang and Lan algorithm (Ref. 25), and Eriksson and Allie algorithm (Ref. 24).

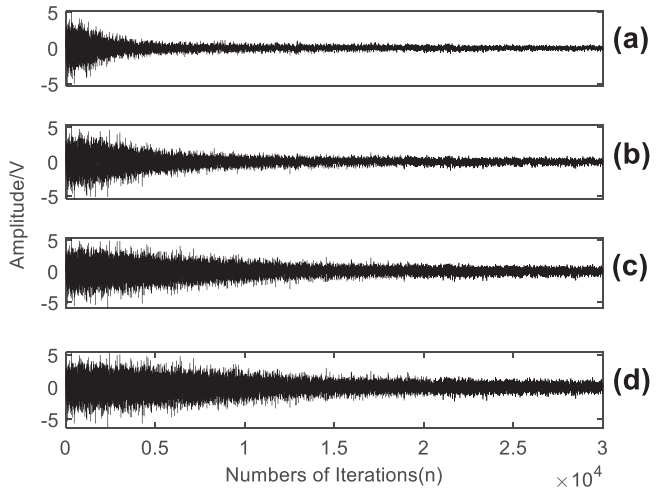

FIG. 12. The relationship between error signal $e(n)$ and number of iterations. (a) The proposed algorithm, (b) Dong *et al.* (Ref. 34) algorithm, (c) Zhang and Lan (Ref. 25) algorithm, and (d) Eriksson and Allie algorithm (Ref. 24).

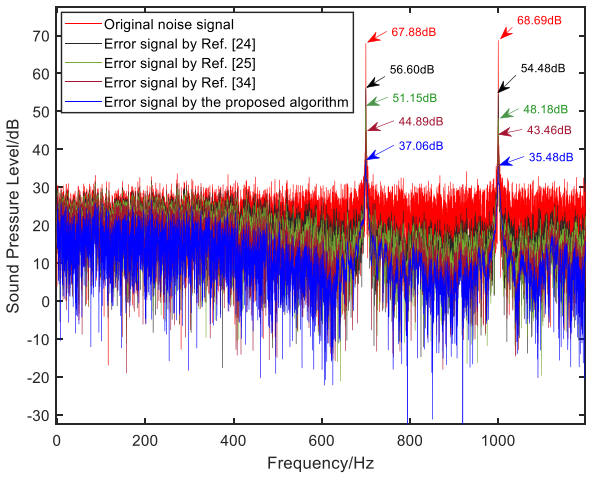

FIG. 14. (Color online) A comparison of the noise control performance using various algorithms.

frequency response of the virtual acoustic feedback path estimated by the algorithm presented by Aslam *et al.*[18] has a large deviation away from that of the real feedback path at low frequencies which can lead to a poor noise control output. Figure 11(b) shows the frequency response of the virtual secondary path $\hat{\mathbf{S}}_1(z)$ calculated by the proposed ANC system with the optimized secondary path identification algorithm. Also, shown in the figure are the frequency response of the real secondary path $\mathbf{S}(z)$ and those estimated using the algorithms presented by Dong *et al.*,[34] Zhang and Lan,[25] and Eriksson and Allie,[24] [$\hat{\mathbf{S}}_2(z)$, $\hat{\mathbf{S}}_3(z)$ and $\hat{\mathbf{S}}_4(z)$, respectively]. It is shown that the proposed algorithm can yield a closely match frequency response to that of the real secondary path so that the delay when a control signal passing the secondary path can be accurately estimated and compensated for a good control outcome. It is noted that a good match frequency response, i.e., $\hat{\mathbf{S}}_2(z)$, can also be produced by using the normalized least mean square (NLMS) algorithm presented by Dong *et al.*,[34] though the matching result is not as good as that using the current approach. The frequency response, $\hat{\mathbf{S}}_4(z)$, estimated using the traditional LMS algorithm,[24] will render a large error compared to the actual frequency response of the secondary path leading to an unstable control system and a poor control result.

Figure 12 compares the convergence speed of the proposed algorithm and the three previously-mentioned algorithms as a function of the number of iterations. It is shown once again that the proposed algorithm has the fastest convergence rate than the other three indicating that the proposed algorithm is highly computation efficient.

Figure 13 compares the spectrograms of the input noise signal and the control output error signals using the proposed algorithm and those of Dong *et al.*,[34] Zhang and Lan,[25] and Eriksson and Allie.[24] It is shown in Fig. 13(b) that the signal energies of the two tonal frequency components at 700 and 1000 Hz are quickly reduced to a small level after less than 0.5 s using the proposed algorithm. Whereas the algorithm proposed by Dong *et al.*[34] takes a much longer time (around 1.3 s) to converge in addition to a higher residual noise, it takes about 2 s for the system to converge using the Zhang and Lan[25] algorithm as well as a poorer control performance. It takes about 3 s for the control system using the LMS algorithm[24] to converge due to the interference of the active control filter and the secondary path identification filter.

Figure 14 compares the sound pressure spectra of the input noise signal and the output error signals using the

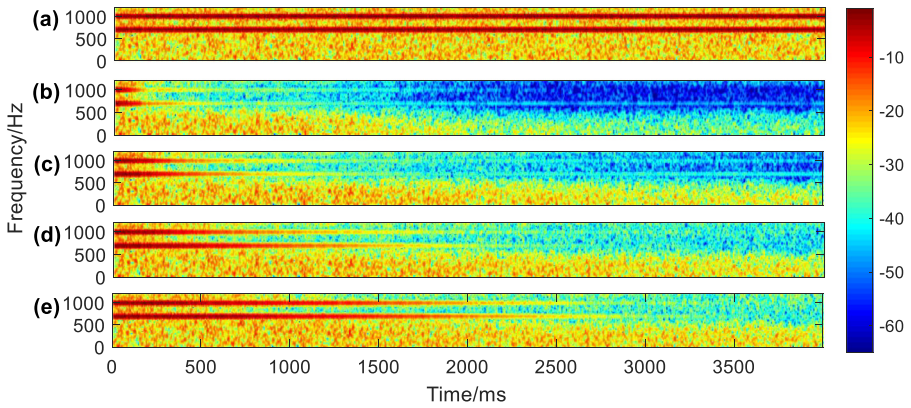

FIG. 13. (Color online) A comparison of the spectrograms of the input and output signals, (a) the input noise signal, (b) the proposed algorithm, (c) Dong *et al.* (Ref. 34) algorithm, (d) Zhang and Lan (Ref. 25)algorithm, and the (e) Eriksson and Allies (Ref. 24) algorithm.

https://doi.org/10.1121/10.0022574

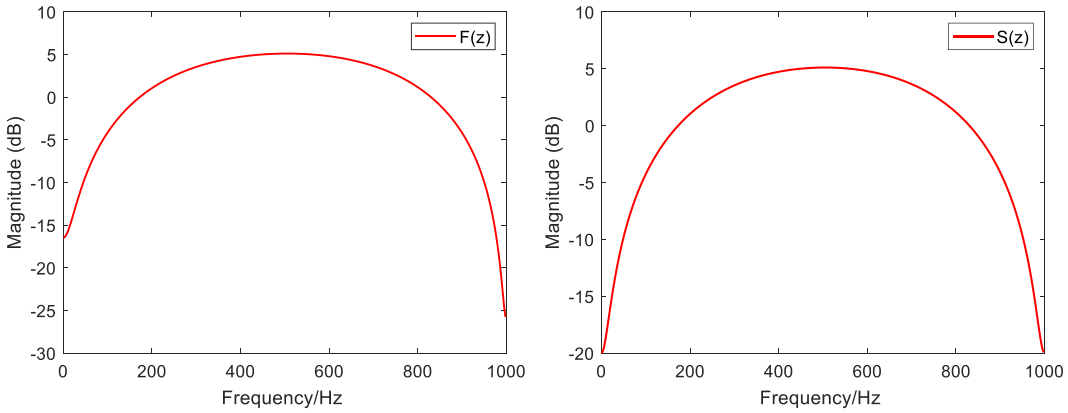

FIG. 15. (Color online) Frequency response curves, (a) the acoustic feedback path (b) the secondary path.

proposed algorithm and the other three algorithms. It is shown that the original sound pressure levels (67.88 and 68.69 dB) of the noise components at 700 and 1000 Hz have been successfully reduced to 37.06 and 35.48 dB, respectively, using the proposed algorithm. The control outcome using the Dong *et al.*,[34] Zhang and Lan,[25] and Eriksson and Allie[24] algorithms is not as good. The result indicates that the proposed algorithm has a superior performance on the mid-frequency noise control on multi-component input noise signal.

To verify the robustness of the proposed control system, the transfer functions of the acoustic feedback path $\mathbf{F}(z)$ and the secondary path $\mathbf{S}(z)$ as depicted by Fig. 11 were changed to that shown in Fig. 15 after 30 000 iterations, and the relative compensation error and relative identification error are calculated.

Figure 16 compares the calculated relative compensation error of the acoustic feedback path using the proposed algorithm and that of Aslam *et al.*[18] as a function of the number of iterations. It is shown that the proposed algorithm renders a smaller relative compensation error than that of Aslam *et al.*,[18] in addition to a much faster convergence speed regardless of the change of the transfer function during the iteration. Figure 17 compares the relative identification error of the secondary path using the proposed algorithm and those using the Dong *et al.*,[34] Zhang and Lan,[25] and Eriksson and Allie[24] algorithms. It is shown that the proposed algorithm has a good anti-interference capacity than the other three due to the use of the adjustment weight factor $\sqrt{\sigma^2_{v_x}(n)/\sigma^2_{v_{g1}}(n)}$.

C. Case 3

A broadband Gaussian white noise with the power of 5dBW as shown in Fig. 18(a) is used in this case study. The signal is filtered first using a bandpass filter of the bandwidth between 300 and 500 Hz as shown in Fig. 18(b), which is then used as the input signal for the proposed ANC system.

Figure 19 compares the frequency spectra of the control output signal using the ANC algorithm presented by Aslam *et al.*[18] and the proposed algorithm where the filter broadband noise signal is used as the input noise. Also, shown in the figure is the frequency spectrum of the filtered signal for comparison. It is shown that the proposed algorithm can achieve a much better control outcome for the filtered broadband signal with more than 20 dB reduction across the

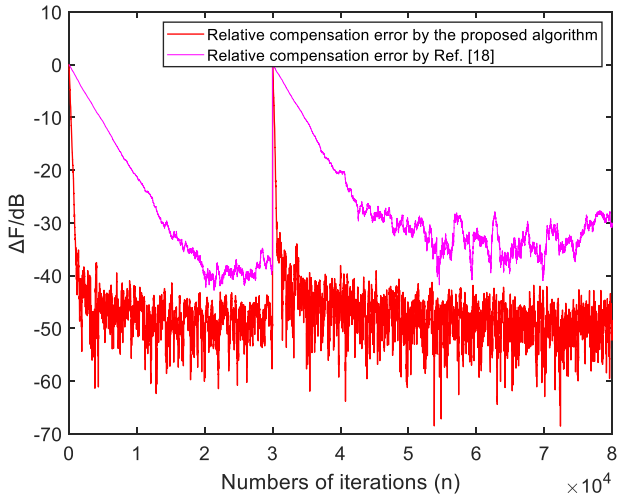

FIG. 16. (Color online) Acoustic feedback path compensation error.

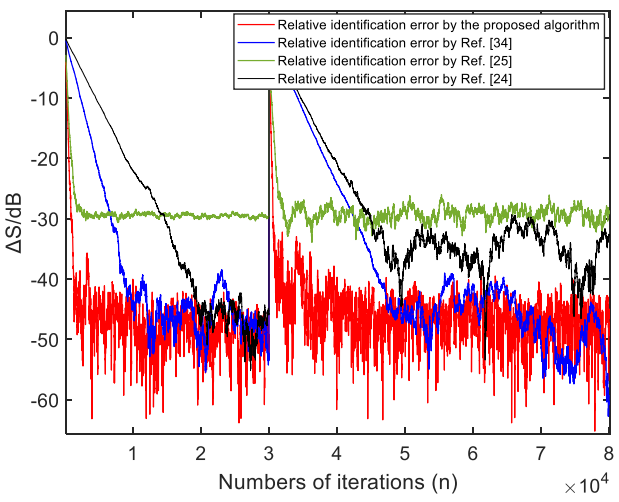

FIG. 17. (Color online) Secondary path identification error.

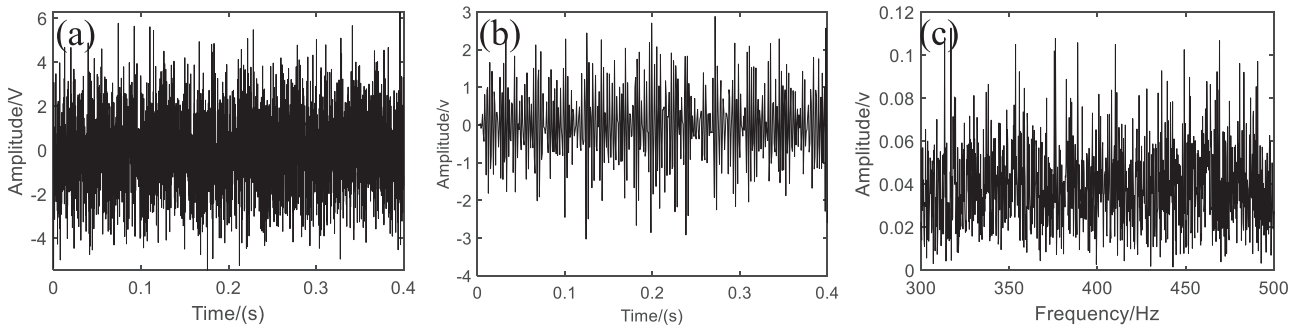

FIG. 18. The simulated input noise signal $r(t)$, (a) the original time waveform, (b) the time waveform of the filtered signal, and (c) the frequency spectrum of the filtered signal.

bandwidth. On the contrary, the algorithm presented by Aslam *et al.*[18] renders a poorer control outcome.

VIII. AN ANALYSIS OF THE COMPUTATION COMPLEXITY

The computation complexity of an ANC algorithm depends upon the amount of addition and multiplication used in the algorithm.[2,3] Table I compares the number of additions and multiplications of the second path identification used by the proposed algorithm and other ANC algorithms. Compared to the algorithm presented by Eriksson and Allie,[24] the computation complexity of the proposed algorithm does increase slightly, though the convergence speed increases substantially besides a much accurate control outcome as shown in Fig. 6. On the other hand, it is shown in the table that the proposed algorithm is less complexity than the algorithms presented by Zhang and Lan[25] and Dong *et al.*[34] judging by the total number of additions and multiplications in addition to the benefits of a fast convergence and a more accurate control outcome.

Note that the word, maximum in the tables implies all filters in the algorithm are used during the acoustic feedback path compensation and the secondary path identification, and the word, minimum implies that only the control filter $\mathbf{W}(n)$ is used when the acoustic feedback path compensation and the secondary path identification are completed.

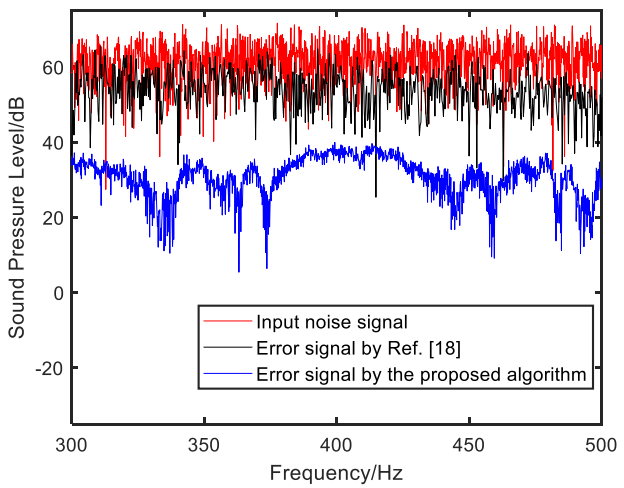

FIG. 19. (Color online) A comparison of the noise control performance using various algorithms.

Table II compares the computation complexity of the acoustic feedback path compensation used by the proposed algorithm and that of Aslam *et al.*[18] It is shown that the proposed algorithm can render a better convergence speed and a better control outcome (see Figs. 4 and 19) than those of the latter algorithm with far fewer additions and multiplications.

IX. CONCLUSION

In this paper, an adaptive variable step-size algorithm was proposed to improve the convergence speed and the noise control outcome of a feedforward ANC system. An adaptive adjusting weight factor was introduced in the proposed algorithm where the gain of the system can be adjusted dynamically during the iteration based on the system convergence to reduce the interference of the injected auxiliary noise on the acoustic feedback loop of the control system. At the same time, an adaptive variable step-size noise cancelation filter was proposed to replace the linear predictive filter to improve the robustness and stability of the control loop of the system. The adaptive algorithm was also used in the secondary path identification to eliminate the interference between the filters where only two filters are needed for a better convergence speed and a more accurate path identification.

The effectiveness of the proposed algorithm and the control system was evaluated using two input multi-components signals and a broadband Gaussian white noise

TABLE I. Computation complexity of the secondary path identification used various ANC algorithms.

ANC algorithm	Additions	Multiplications
Eriksson and Allie (Ref. 24)	$2L_s + 3L_w - 1$	$2L_s + 3L_w + 2$
Zhang and Lan (Ref. 25)	$3L_s + 4L_w + 3L_N + 3$	$3L_s + 4L_w + L_N + 12$
Dong *et al.*(Ref. 34)	$6L_s + 2L_w - 2$	$6L_s + 2L_w + 6$
Proposed algorithm		
Maximum[a]	$3L_s + 2L_w + 3L_i$	$3L_s + 2L_w + 2L_i + 2$
Minimum[b]	$2L_s + 2L_w + L_i$	$2L_s + 2L_w + L_i + 1$

[a]Filters $\hat{\mathbf{S}}(n)$, $\mathbf{d}(n)$, $\mathbf{i}(n)$ and $\mathbf{w}(n)$.
[b]Only filter $\mathbf{w}(n)$ is updated.

https://doi.org/10.1121/10.0022574

TABLE II. Computation complexity of the acoustic feedback compensation used various ANC algorithms.

ANC algorithm	Additions	Multiplications
Aslam *et al.* (Ref. 18)		
Maximum	$5L_f + 4L_w + L_s + 4L_b + 11$	$5L_f + 4L_w + L_s + 4L_b + 22$
Minimum	$5L_f + 2L_w + L_s + L_b$	$L_f + 2L_w + L_s + L_b + 5$
Proposed algorithm		
Maximum[a]	$5L_f + 2L_w + L_s + 3L_h + 3$	$5L_f + 2L_w + L_s + 2L_h + 9$
Minimum[b]	$3L_f + 2L_w + L_s + L_h + 3$	$L_f + 2L_w + L_s + L_h + 5$

[a]Filters $\hat{\mathbf{f}}(n)$, $\mathbf{h}(n)$, and $\mathbf{w}(n)$.
[b]Only filter $\mathbf{w}(n)$ is updated.

signal, and the results were compared to those obtained using those commonly employed ANC algorithms. It was shown that the proposed algorithm does not only have a faster convergence speed, it also has a smaller residual noise after the control comparing to other similar ANC algorithms.

ACKNOWLEDGMENTS

Financial support from the Department of Science and Technology of Shandong Provincial Government through the Innovative Project Grant (Project No: YDZX2022111) and the 111 project from the Ministry of Science and Technology of China (D21017) for this work are gratefully acknowledged.

AUTHOR DECLARATIONS

Conflict of Interest

The authors declare that they have no known competing financial interests or personal relationships that could have appeared to influence the work reported in this paper.

DATA AVAILABILITY

Data used in the paper will be made available upon requested.

APPENDIX A

The detailed derivation of Eq. (17) is given as follows:

$$\begin{aligned}&\mathrm{E}\left[e(n)e(n-\Delta)\right]\\&=\mathrm{E}\left[\left(d(n)+s(n)*\left(y_t(n)+v_{g2}(n)\right)\right)\right.\\&\quad\times\left(d(n-\Delta)+s(n-\Delta)\right.\\&\quad\left.\left.*\left(y_t(n-\Delta)+v_{g2}(n-\Delta)\right)\right)\right].\end{aligned}\tag{A1}$$

Substituting Eq. (6) into Eq. (A1), we have

$$\begin{aligned}&\mathrm{E}\left[e(n)e(n-\Delta)\right]\\&=\mathrm{E}\left[\left(d(n)+s(n)*\left(\left(y(n)+v_{g1}(n)\right)+v_{g2}(n)\right)\right)\right.\\&\quad\times\left(d(n-\Delta)+s(n-\Delta)\right.\\&\quad\left.\left.*\left(y(n-\Delta)+v_{g1}(n-\Delta)+v_{g2}(n-\Delta)\right)\right)\right].\end{aligned}\tag{A2}$$

Letting $d(n)+s(n)*y(n)=k(n)$ and $v_{g1}(n)+v_{g2}(n)=v(n)$, we have

$$\begin{aligned}&\mathrm{E}\left[e(n)e(n-\Delta)\right]\\&=\mathrm{E}\left[\left(k(n)+s(n)*v(n)\right)\left(k(n-\Delta)+s(n)*v(n-\Delta)\right)\right]\\&=\mathrm{E}\left[k(n)k(n-\Delta)\right]+\mathrm{E}\left[k(n)s(n)*v(n-\Delta)\right]\\&\quad+\mathrm{E}\left[k(n-\Delta)s(n)*v(n)\right]+\mathrm{E}\left[s(n)*v(n)s(n)*v(n-\Delta)\right].\end{aligned}\tag{A3}$$

Removing the uncorrelated product terms in Eq. (A3), we have

$$\begin{aligned}&\mathrm{E}\left[e(n)e(n-\Delta)\right]\\&=\mathrm{E}\left[k(n)k(n-\Delta)\right]+\mathrm{E}\left[s(n)*v(n)s(n)*v(n-\Delta)\right]\\&=\mathrm{E}\left[k(n)k(n-\Delta)\right]+\sum_{i=0}^{L_s-1}s_i(n)\sum_{j=0}^{L_s-1}s_j(n)\\&\quad\times\mathrm{E}\left[v(n-i)v(n-j-\Delta)\right].\end{aligned}\tag{A4}$$

APPENDIX B

A detailed derivation of Eq. (52a) is given as follows. Substituting Eq. (47) into Eq. (25), we have

$$e_f(n)=\mathbf{v}_{g1}^T(n)\mathbf{m}_f(n)+v_x(n).\tag{B1}$$

Substituting Eq. (B1) into Eq. (51) and removing the uncorrelated product terms,

$$\begin{aligned}&\mathrm{E}\left[\mathbf{v}_{g1}^T(n-1)\mathbf{m}_f(n-1)e_f(n-1)\right]\\&=\mathrm{E}\left[\mathbf{v}_{g1}^T(n-1)\mathbf{m}_f(n-1)\mathbf{v}_{g1}^T(n-1)\mathbf{m}_f(n-1)\right]\\&=\mathrm{E}\left[\left(\mathbf{v}_{g1}^T(n-1)\mathbf{m}_f(n-1)\right)^2\right].\end{aligned}\tag{B2}$$

According to the independence assumption that $\mathbf{v}_{g1}^T(n)$ and $\mathbf{m}_f(n)$ are independent of each other, Eq. (B2) can be rewritten as Aslam *et al.*,[18]

$$\begin{aligned}&\mathrm{E}\left[\left(\mathbf{v}_{g1}^T(n-1)\mathbf{m}_f(n-1)\right)^2\right]\\&=\mathrm{E}\left\{\mathrm{tr}\left[\mathbf{m}_f^T(n-1)\mathbf{m}_f(n-1)\right]\mathbf{R}_{\mathbf{v}_{g1}\mathbf{v}_{g1}^T}\right\}\\&=\mathrm{tr}\left\{\mathrm{E}\left[\mathbf{m}_f^T(n-1)\mathbf{m}_f(n-1)\right]\mathbf{R}_{\mathbf{v}_{g1}\mathbf{v}_{g1}^T}\right\},\end{aligned}\tag{B3}$$

where $\mathbf{R}$ stands for the autocorrelation matrix, $\mathbf{R}_{\mathbf{v}_{g1}\mathbf{v}_{g1}^T}=\mathrm{E}\left[\mathbf{v}_{g1}(n)\mathbf{v}_{g1}^T(n)\right]$, and tr[·] represents the trace of a matrix.

Using a mathematical operation similar to Eq. (32), Eq. (B2) can be simplified to

$$\begin{aligned}&\mathrm{E}\left[\mathbf{v}_{g1}^T(n-1)\mathbf{m}_f(n-1)e_f(n-1)\right]\\&=\sigma_{v_{g1}}^2\mathrm{E}\left[\|\mathbf{m}_f(n-1)\|_2^2\right].\end{aligned}\tag{B4}$$

The last term in Eq. (51) can now be simplified to

$$\begin{aligned}
&\mathrm{E}\left[e_f^2(n-1)\mathbf{v}_{g1}^T(n-1)\mathbf{v}_{g1}(n-1)\right] \\
&\quad = \mathrm{tr}\left\{\mathrm{E}\left[e_f^2(n-1)\mathbf{v}_{g1}(n-1)\mathbf{v}_{g1}^T(n-1)\right]\right\} \\
&\quad = \mathrm{tr}\left\{\mathrm{E}\left[\left(\mathbf{v}_{g1}^T(n-1)\mathbf{m}_f(n-1)+v_x(n-1)\right)^2\right.\right. \\
&\qquad \left.\left.\times\, \mathbf{v}_{g1}(n-1)\mathbf{v}_{g1}^T(n-1)\right]\right\}. \qquad \text{(B5)}
\end{aligned}$$

Expanding the perfect square term in Eq. (B5), we have

$$\begin{aligned}
&\mathrm{tr}\left\{\mathrm{E}\left[\left(\mathbf{v}_{g1}^T(n-1)\mathbf{m}_f(n-1)+v_x(n-1)\right)^2\right.\right. \\
&\qquad \left.\left.\times\, \mathbf{v}_{g1}(n-1)\mathbf{v}_{g1}^T(n-1)\right]\right\} \\
&\quad = \mathrm{tr}\left\{\mathrm{E}\left[\mathbf{v}_{g1}(n-1)\mathbf{v}_{g1}^T(n-1)\mathbf{m}_f(n-1)\right.\right. \\
&\qquad \times\, \mathbf{m}_f^T(n-1)\mathbf{v}_{g1}(n-1)\mathbf{v}_{g1}^T(n-1) \\
&\qquad \left.+\, 2\mathbf{v}_{g1}^T(n-1)\mathbf{m}_f(n-1)\right]v_x(n-1) \\
&\qquad \times\, \mathbf{v}_{g1}(n-1)\mathbf{v}_{g1}^T(n-1)+v_x^2(n-1) \\
&\qquad \left.\times\, \mathbf{v}_{g1}(n-1)\mathbf{v}_{g1}^T(n-1)\right\} \\
&\quad = \mathrm{tr}\left\{\mathrm{E}\left[\mathbf{v}_{g1}(n-1)\mathbf{v}_{g1}^T(n-1)\mathbf{m}_f(n-1)\right.\right. \\
&\qquad \times\, \mathbf{m}_f^T(n-1)\mathbf{v}_{g1}(n-1)\mathbf{v}_{g1}^T(n-1)\left.\right] \\
&\qquad \left.+\, E\left[v_x^2(n-1)\mathbf{v}_{g1}(n-1)\mathbf{v}_{g1}^T(n-1)\right]\right\}. \qquad \text{(B6)}
\end{aligned}$$

Simplifying the last term in Eq. (B6), and letting $\mathbf{m}_f(n-1)\mathbf{m}_f^T(n-1)=\mathbf{D}(n-1)$, we have

$$\begin{aligned}
&\mathrm{tr}\left\{\mathrm{E}\left[\mathbf{v}_{g1}(n-1)\mathbf{v}_{g1}^T(n-1)\mathbf{m}_f(n-1)\right.\right. \\
&\qquad \times\, \mathbf{m}_f^T(n-1)\mathbf{v}_{g1}(n-1)\mathbf{v}_{g1}^T(n-1)\left.\right] \\
&\qquad \left.+\, E\left[v_x^2(n-1)\mathbf{v}_{g1}(n-1)\mathbf{v}_{g1}^T(n-1)\right]\right\} \\
&\quad = \mathrm{tr}\left\{\mathrm{E}\left[\mathbf{v}_{g1}(n-1)\mathbf{v}_{g1}^T(n-1)\mathbf{D}(n-1)\right.\right. \\
&\qquad \left.\left.\times\, \mathbf{v}_{g1}(n-1)\mathbf{v}_{g1}^T(n-1)\right]\right\}+L_f\sigma_{v_{g1}}^2\sigma_x^2. \qquad \text{(B7)}
\end{aligned}$$

Using the approach given by Farhang-Boroujeny,[33] the first term in Eq. (B7) can be simplified to yield

$$\begin{aligned}
&\mathrm{E}\left[\mathbf{v}_{g1}(n-1)\mathbf{v}_{g1}^T(n-1)\mathbf{D}(n-1)\mathbf{v}_{g1}(n-1)\mathbf{v}_{g1}^T(n-1)\right] \\
&\quad = 2\Lambda\mathbf{D}(n-1)\Lambda+\mathrm{tr}[\Lambda\mathbf{D}(n-1)]\Lambda \\
&\quad = \sigma_{v_{g1}}^4\mathrm{E}\left[\|\mathbf{m}_f(n-1)\|_2^2\right]\mathbf{I}_{L_f} \\
&\qquad +\, 2\sigma_{v_{g1}}^4\mathrm{E}\left[\mathbf{m}_f(n-1)\mathbf{m}_f^T(n-1)\right], \qquad \text{(B8)}
\end{aligned}$$

where $\mathrm{E}\left[\mathbf{v}_{g1}(n-1)\mathbf{v}_{g1}^T(n-1)\right]=\Lambda$, $\mathbf{I}_{L_f}$ is an identity matrix of order L_f.

Substituting Eq. (B8) into Eq. (B7), we have

$$\begin{aligned}
&\mathrm{E}\left[e_f^2(n-1)\mathbf{v}_{g1}^T(n-1)\mathbf{v}_{g1}(n-1)\right] \\
&\quad = \mathrm{tr}\left\{\sigma_{v_{g1}}^4\mathrm{E}\left[\|\mathbf{m}_f(n-1)\|_2^2\right]I_{L_f}\right. \\
&\qquad \left.+\, 2\sigma_{v_{g1}}^4\mathrm{E}\left[\mathbf{m}_f(n-1)\mathbf{m}_f^T(n-1)\right]\right\}+L_f\sigma_{v_{g1}}^2\sigma_x^2 \\
&\quad = (L_f+2)\sigma_{v_{g1}}^4\mathrm{E}\left[\|\mathbf{m}_f(n-1)\|_2^2\right]+L_f\sigma_{v_{g1}}^2\sigma_x^2. \qquad \text{(B9)}
\end{aligned}$$

[1] D. Kim, V. Saravanan, H. Kim, T. Yuk, and S. Lee, "Development of active noise control simulation with virtual controller based on computational aerocoustics," J. Acoust. Soc. Am. **153**, 2789–2802 (2003).

[2] S. M. Kuo and D. Morgan, *Active Noise Control Systems: Algorithms and DSP Implementations* (Wiley, New York, 1996).

[3] C. H. Hansen, *Understanding Active Noise Cancellation* (CRC Press, London, 2001).

[4] L. C. Liu, S. Gujjula, P. Thanigai, and S. M. Kuo, "Still in womb: Intrauterine acoustic embedded active noise control for infant incubators," Adv. Acoust. Vib. **2008**, 495317.

[5] M. Kida, R. Hirayama, Y. Kajikawa, T. Tani, and Y. Kurumi, "Head-mounted active noise control system for MR noise," in *ICASSP'09 Proceedings of the 2009 IEEE International Conference on Acoustics, Speech and Signal Processing*, Taipei, Taiwan (April 19–24, 2009), pp. 245–248.

[6] N. Devineni, I. Panahi, and P. Kasbekar, "Predictive multi-channel feedback active noise control for HVAC systems," in *2011 IEEE International Conference on Electro/Information Technology*, Mankato, MN (May 15–17, 2011), pp. 1–5.

[7] D. Ding, P. S. Wang, and Y. M. Wang, "An active noise control filter design method based on machine learning algorithms," J. Acoust. Soc. Am. **152**, A99 (2022).

[8] M. S. Aslam and M. A. Raja, "A new adaptive strategy to improve online secondary path modeling in active noise control systems using fractional signal processing approach," Signal Process. **107**, 433–443 (2015).

[9] M. S. Aslam, P. Shi, and C. C. Lim, "Variable threshold-based selective updating algorithms in feed-forward active noise control systems," IEEE Trans. Circuits Syst. I **66**(2), 782–795 (2019).

[10] S. Ahmed and M. T. Akhtar, "Gain scheduling of auxiliary noise and variable step-size-size for online acoustic feedback cancellation in narrowband active noise control systems," IEEE/ACM Trans. Audio. Speech. Lang. Process. **25**(2), 333–343 (2017).

[11] Z. Mehmood, M. Tufail, and S. Ahmed, "A new variable step-size size method for online feedback path modeling in active noise control systems," in *Proceedings of the 13th IEEE International Multitopic Conference*, Islamabad, Pakistan (December 14–15, 2009), pp. 01–06.

[12] L. L. J. Sun and B. Huang, "A novel feedback active noise control for broadband chaotic noise and random noise," Appl. Acoust. **116**(15), 229–237 (2017).

[13] C. E. Warnaka, L. A. Poole, and J. Tichy, "Active acoustic attenuators," U.S. patent 447390 (1984).

[14] S. Ahmed, M. T. Akhtar, and X. Zhang, "Online acoustic feedback mitigation with improved noise-reduction performance in active noise control systems," IET Signal Process. **7**(6), 505–514 (2013).

[15] M. T. Akhtar and W. Mitsuhashi, "Variable step-size-size based method for acoustic feedback modeling and neutralization in active noise control systems," Appl. Acoust. **72**(5), 297–304 (2011).

[16] S. M. Kuo and J. Luan, "On-line modeling and feedback compensation for multiple-channel active noise control systems," Appl. Signal Process. **1**(2), 64–75 (1994).

[17] S. Ahmed, M. T. Akhtar, and X. Zhang, "Variable step-size-size based-adaptive algorithm for acoustic feedback cancellation during online operation of ANC systems," in *Proceedings of the IEEE China Summit and International Conference on Signal and Information Processing*, Chendgu, China (July 12–15, 2015), pp. 74–78.

[18] M. S. Aslam, P. Shi, and C. C. Lim, "Self-adapting variable step-size size strategies for active noise control systems with acoustic feedback," Automatica **123**, 109354 (2021).

[19] M. T. Akhtar, M. Abe, and M. Kawamata, "On active noise control systems with online acoustic feedback path modeling," IEEE Trans. Audio Speech Lang. Process. **15**(2), 593–600 (2007).

[20]Y. Z. Zhuang and Y. Liu, "A numerically stable constrained optimal filter designer method for multichannel active noise control using dualconic formulation," J. Acoust. Soc. Am. **152**, 2169–2182 (1998).
[21]L. A. Poole, G. E. Warnaka, and R. C. Cutter, "The implementation of digital filters using a modified Widrow-Hoff algorithm for the adaptive cancellation of acoustic noise," in *Proceedings of the IEEE International Conference on Acoustics, Speech, and Signal Processing*, San Diego, CA (March 19–21, 1984).
[22]W. C. Niu, C. Z. Zou, B. Li, and W. Wang, "Adaptive vibration suppression of time-varying structures with enhanced FxLMS algorithm," Mech. Syst. Signal Process. **118**, 93–107 (2019).
[23]B. Q. Wu and M. Bodson, "Multi-channel active noise control for periodic sources-indirect approach," Automatica **40**, 203–212 (2004).
[24]L. J. Eriksson and M. C. Allie, "Use of random noise for on-line transducer modeling in an adaptive active attenuation system," J. Acoust. Soc. Am. **85**, 797–802 (1989).
[25]M. Zhang and H. Lan, "Cross-updated active noise control system with online secondary path modeling," IEEE Trans. Speech Audio Process. **9**, 598–602 (2001).
[26]S. M. Kuo and D. Vijayan, "A secondary path modeling technique for active noise control systems," IEEE Trans. Speech Audio Process. **5**, 374–377 (1997).
[27]C. Bao, P. Sas, and H. V. Brussel, "Comparison of two-on-line identification algorithms for active noise control," in *Proceedings of the Conference on Recent Advances in Active Control of Sound and Vibration*, Blacksburg, VA (April 28–30, 1993), pp. 38–54.
[28]M. Zhang and H. Lan, "On comparison of online secondary path modeling methods with auxiliary noise," IEEE Trans. Speech Audio Process. **13**, 618–628 (2005).
[29]M. T. Akhtar, M. Abe, and M. Kawamata, "Noise power scheduling inactive noise control systems with online secondary path modeling," IEICE Electron. Express **4**, 66–71 (2007).
[30]S. Y. Wang, L. Gu, F. Liu, and M. M. Dong, "Online secondary path modeling for active sound quality control systems," Appl. Acoust. **155**, 44–52 (2019).
[31]J. Benesty and S. Member, "A nonparametric VSS NLMS algorithm," IEEE Signal Process. Lett. **13**, 581–584 (2006).
[32]W. A. Gardner, "Learning characteristics of stochastic gradient descent algorithm: A general study, analysis and critique," Signal Process. **6**, 113–133 (1984).
[33]B. Farhang-Boroujeny, *Adaptive Filters: Theory and Applications,* 2nd ed. (Wiley, New York, 2013).
[34]W. K. Dong, W. H. Jun, and P. Poogyeon, "Two-stage active noise control with online secondary-path filter based on an adapted scheduled-step size NLMS algorithm," Appl. Acoust. **158**, 107031 (2020).